Magnetic Coupling of $Gd_3N@C_{80}$ Endohedral Fullerenes to a Substrate

Christian F. Hermanns,[1] Matthias Bernien,[1] Alex Krüger,[1] Christian Schmidt,[1] Sören T. Waßerroth,[1] Gelavizh Ahmadi,[1] Benjamin W. Heinrich,[1] Martin Schneider,[2] Piet W. Brouwer,[2] Katharina J. Franke,[1] Eugen Weschke,[3] and Wolfgang Kuch[1,*]

[1]*Institut für Experimentalphysik, Freie Universität Berlin, Arnimallee 14, 14195 Berlin, Germany*
[2]*Institut für Theoretische Physik and Dahlem Center for Complex Quantum Systems, Freie Universität Berlin, Arnimallee 14, 14195 Berlin, Germany*
[3]*Helmholtz-Zentrum Berlin für Materialien und Energie, Albert-Einstein-Straße 15, 12489 Berlin, Germany*

(Received 18 June 2013; published 15 October 2013)

Using magnetic endohedral fullerenes for molecular spintronics requires control over their encapsulated magnetic moments. We show by field-dependent x-ray magnetic circular dichroism measurements of $Gd_3N@C_{80}$ endohedral fullerenes adsorbed on a Cu surface that the magnetic moments of the encapsulated Gd atoms lie in a $4f^7$ ground state and couple ferromagnetically to each other. When the molecules are in contact with a ferromagnetic Ni substrate, we detect two different Gd species. The more abundant one couples antiferromagnetically to the Ni, whereas the other one exhibits a stronger and ferromagnetic coupling to the substrate. Both of these couplings to the substrate can be explained by an indirect exchange mechanism mediated by the carbon cage. The origin of the distinctly different behavior may be attributed to different orientations and thus electronic coupling of the carbon cage to the substrate, as revealed by scanning tunneling microscopy of the fullerenes on Cu.

DOI: 10.1103/PhysRevLett.111.167203 PACS numbers: 75.70.−i, 33.15.Kr, 75.30.Et, 78.70.Dm

The discovery of Buckminster fullerenes [1] has led to the idea of encapsulating different types of atoms inside these chemical compounds like single magnetic rare-earth atoms [2], noble gases [3], and nonmetal atoms such as nitrogen [4]. These endohedral fullerenes [5] can even contain whole rare-earth metal nitride clusters [6]. The carbon cages isolate encapsulated reactive magnetic species from aggressive environments and confine, in the case of trimetallic nitride endohedral fullerenes, three rare-earth ions in a relatively small space. Long magnetic relaxation times, characteristic of single-molecule magnets, have been observed in $DySc_2N@C_{80}$ endohedral fullerenes [7]. Endohedral fullerenes are hence promising candidates for molecular spintronics. However, a reliable communication with and access to their enclosed magnetic units without the need for an applied magnetic field is still an ongoing field of research [8]. Interesting in this context is a reported antiferromagnetic (AFM) coupling between the encapsulated magnetic moments and the electrons situated on the carbon cage [9]. Additionally, a ferromagnetic (FM) spin coupling between endohedral metallofullerenes and a cyclodimeric copper porphyrin has been observed [10], which goes beyond a reported internal spin coupling of different magnetic moments within the carbon cage [7,11].

A magnetic coupling to a substrate as a means to stabilize paramagnetic molecules against thermal fluctuations has been observed for different metalloporphyrin molecules adsorbed on FM surfaces [12–14]. The magnetic interaction of endohedral fullerenes, on the other hand, with a magnetic electrode has not yet been reported. Here, we show by temperature-, field-, and angle-dependent x-ray magnetic circular dichroism (XMCD) measurements combined with scanning tunneling microscopy (STM) that the three Gd $4f$ magnetic moments inside $Gd_3N@C_{80}$ endohedral fullerenes [inset of Fig. 1(b)] couple ferromagnetically with each other, and that furthermore the adsorption on FM Ni films leads to a substrate-induced ordering of these moments due to a substrate-molecule exchange interaction across the carbon cage. Our measurements can be explained in terms of two electronically different types of Gd atoms in the fullerenes on the surface, both having a $4f^7$ electronic configuration. The majority species couples antiferromagnetically to the substrate magnetization, while the minority species couples ferromagnetically. The Gd net magnetization is antiparallel to the one of the Ni film at sufficiently low temperatures, while it becomes parallel at higher temperatures, since the coupling of the minority species is stronger.

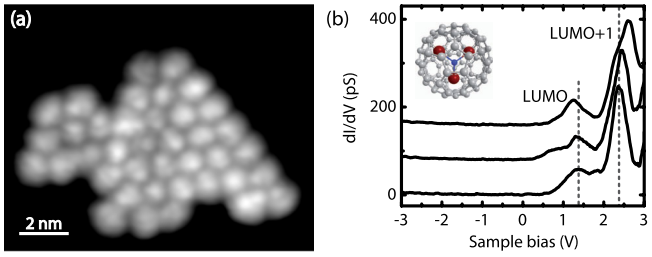

FIG. 1 (color online). $Gd_3N@C_{80}$ on Cu(001). (a) STM constant-current topography of a monolayer island at $V = -0.1$ V and $I = 200$ pA. (b) Characteristic dI/dV spectra on different molecules (feedback loop disabled at 3 V and 200 pA, spectra offset for clarity). Inset: Sketch of the molecule.

STM experiments were performed at 4.8 K under UHV conditions in a homebuilt STM. X-ray absorption (XA) spectroscopy measurements were carried out at the UE46-PGM-1 beam line at the synchrotron radiation source BESSY II in Berlin. The spectra were acquired in total-electron-yield mode in external magnetic fields up to 5.9 T applied along the incidence of the x rays. Ferromagnetic Ni films of 11 monolayer thickness and about 1/10 of a monolayer of $Gd_3N@C_{80}$ were deposited by thermal evaporation onto the substrate held at room temperature.

We first show in Fig. 1 a STM constant-current topograph of $Gd_3N@C_{80}$ on Cu(001). The molecules are found to assemble in small monolayer islands. The molecules exhibit different fine structures with different apparent heights (from 5 to 6.5 Å at −0.1 V sample bias), which is linked to different orientations of the C_{80} cage with respect to the surface [15–18]. In dI/dV spectra we detect molecular resonances related to the lowest unoccupied molecular orbital (LUMO) and LUMO+1 at ∼1.2 and 2.5 V, respectively. These show variations in the energetic position and splitting of the formerly degenerate levels depending on the adsorption geometry.

The line shapes of Gd $M_{4,5}$ XA spectra as well as of the corresponding XMCD difference spectra of $Gd_3N@C_{80}$ on Cu(001) and Ni/Cu(001) exhibit distinctive main peaks at the Gd M_5 edge (Fig. 2). Comparison to literature [19] clearly reveals a $4f^7$ electronic configuration of the Gd atoms. The independence of the XA line shape from the incidence direction is consistent with this assignment and the isotropic distribution of the $4f^7$ electron density. Note that at 0.2 T the Gd XMCD signal is opposite to the one of the Ni substrate, shown in the inset. This proves antiferromagnetic coupling between Ni and Gd, as will be discussed further down.

To probe the magnetic interaction between the Gd ions inside the fullerene, we measure the field-dependent net magnetization M of the molecules on Cu(001) along the surface normal and under 35° incidence, reflected by the Gd $M_{4,5}$ XMCD signal [Fig. 3(a)]. A stronger curvature of the $M(B)$ curve is observed for the latter, suggesting an anisotropic behavior of the Gd spins. Dotted lines are the result of a fit to the data considering paramagnetic moments of size $J = 7/2$ characteristic of a single Gd atom, in combination with uniaxial anisotropy, represented by the zero-field splitting parameter D according to the effective Hamiltonian $\mathcal{H} = \sum_{i=1}^{3}(DJ_{zi}^2 - \mu_B g\mathbf{B}\cdot\mathbf{J_i})$, where μ_B is Bohr's magneton, $g = 2$ the g factor, $\mathbf{B}$ the external magnetic field, $i = 1, 2, 3$ an index labeling the three Gd atoms in the cluster, and $D = 18$ μeV as a result from the fit. The net magnetization M is calculated from the thermal population of the resulting m_J levels. The spin dipole moment T_z is around 5% of the spin moment in the case of Gd [20] assuming atomic $4f$ wave functions, and has been neglected. It is obvious that such a model of noninteracting paramagnetic Gd moments does not satisfactorily describe the experimental data. The larger curvature reveals the existence of intramolecular ferromagnetic coupling J_{Gd}. A simulation including intramolecular exchange, with Hamiltonian $\mathcal{H}_{ex} = -J_{Gd}\sum_{i<j}\mathbf{J}_i\cdot\mathbf{J}_j$, shows good agreement with the data for $J_{Gd} \gtrsim 50$ μeV and $D = 25$ μeV. Simulation results with $J_{Gd} = 50$ μeV and $J_{Gd} = 137$ μeV are shown as dashed and solid curves, respectively. [The values for J_{Gd} of the fits shown in the figure result from simultaneous fits to the data of $Gd_3N@C_{80}$ on both Cu(001) and Ni/Cu(001), as described below.] A magnetic coupling between the Gd atoms inside one fullerene has already been discussed theoretically for isolated $Gd_3N@C_{80}$ molecules [21,22]. Experimentally, a ferromagnetic coupling of about 62 μeV has been deduced from ESR measurements on bulk samples [11], while micro-SQUID experiments pointed towards a weak antiferromagnetic interaction between the Gd ions [23]. We note that hence both essential ingredients for single-molecule-magnet behavior, anisotropy and coupling, are present in $Gd_3N@C_{80}$/Cu(001).

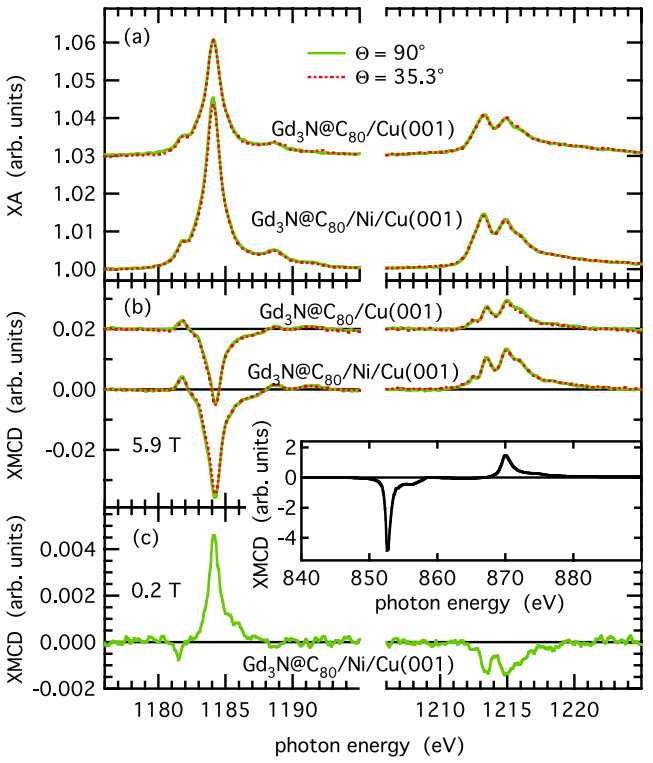

FIG. 2 (color online). Gd $M_{4,5}$ helicity-averaged XA spectra (a) and corresponding XMCD difference spectra (b) of $Gd_3N@C_{80}$ on Cu(001) and Ni/Cu(001), measured at normal incidence (green continuous lines) and at 35° grazing incidence (red dotted lines) with circularly polarized light at 4.5 K in an applied magnetic field of $B = 5.9$ T. (c) XMCD difference spectrum of $Gd_3N@C_{80}$/Ni/Cu(001) measured in an applied field of 0.2 T. Note that the $Gd_3N@C_{80}$ coverages were about 30% different on the two substrates. Note also the different vertical scales in (b) and (c). Inset: XMCD spectrum at the Ni $L_{2,3}$ edges of the $Gd_3N@C_{80}$/Ni/Cu(001) sample.

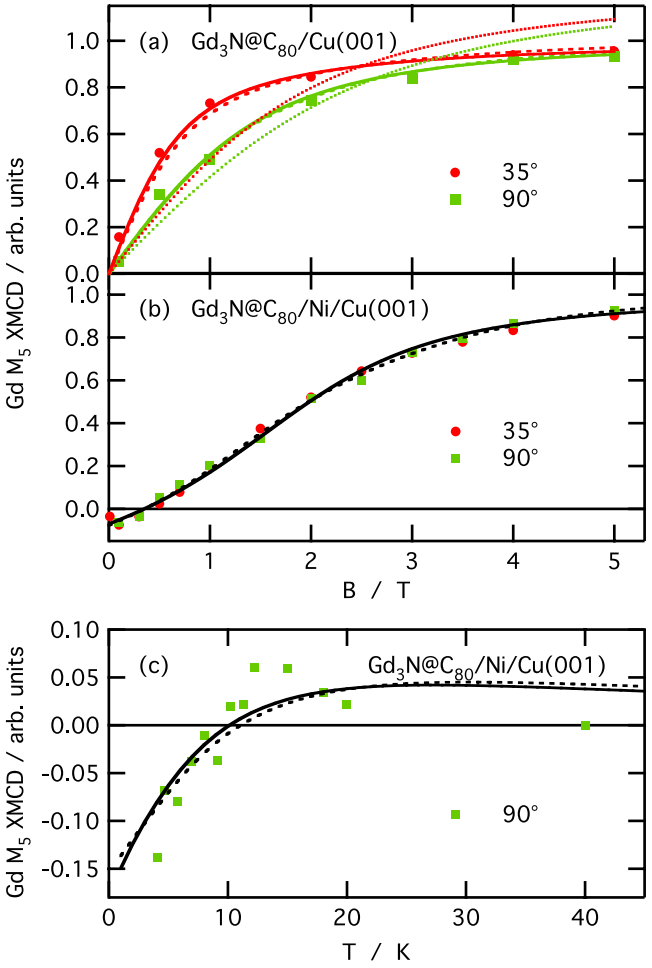

FIG. 3 (color online). Field dependence at $T = 4.5$ K (a),(b) and temperature dependence at $B = 0.01$ T (c) of the relative Gd magnetization, obtained from integrated M_5 edge XMCD spectra, for $Gd_3N@C_{80}/Cu(001)$ (a) and $Gd_3N@C_{80}/Ni/Cu(001)$ (b),(c) taken in normal (green squares) and under 35° grazing incidence (red circles). The dotted line in (a) is the best fit of a model of independent Gd moments, solid and dashed lines in all panels are the results of simultaneous fits to all data using the models described in the text.

To investigate a possible magnetic interaction with a FM substrate, we probe the Gd XMCD signal and its field dependence of the $Gd_3N@C_{80}$ molecules on a Ni substrate. Interestingly, at $B = 0.2$ T and $T = 4.5$ K [Fig. 2(c)] the Gd XMCD signal at the M_5 edge exhibits the opposite sign than at 5.9 T and than the one at the L_3 edge of the Ni $L_{2,3}$ XMCD spectrum of the corresponding sample, shown in the inset of Fig. 2. This means that the net Gd magnetization in this case is oriented opposite to the Ni magnetization and also opposite to the external magnetic field. This proves an overall antiferromagnetic coupling between the Ni magnetization and the Gd spins inside the fullerene cage.

The Ni film has only a moderate out-of-plane anisotropy, such that it can be conveniently saturated in the direction of the external fields [24,25]. The negative XMCD of the Gd M_5 edge at small fields [Fig. 3(b)] shows that for both field directions there is an overall antiparallel coupling between the Gd and the Ni magnetization. Gd moments follow the Ni magnetization for out of plane and in plane. This coupling to the substrate is overcome by a magnetic field larger than about 0.4 T, which is sufficient to align the Gd magnetization with the field parallel to the Ni magnetization at $T = 4.5$ K. The data for normal and grazing orientation of the field are virtually identical, indicating that the coupling is isotropic and that there is also no considerable magnetic anisotropy in this system, in contrast to $Gd_3N@C_{80}/Cu(001)$. The temperature dependence at the very small field of 0.01 T, applied along the surface normal, is shown in Fig. 3(c). Interestingly, there is a crossover to positive values at a temperature of about 10 K. Since the positive XMCD data above 10 K are too large to be caused solely by the external field of 0.01 T [26], the XMCD data cannot be fitted with a single parameter describing the exchange coupling between the Gd magnetic moments and the substrate magnetization that can be considered as constant at these temperatures. Instead, as the simplest more general model, we consider two "species" of Gd atoms, with different and opposite exchange couplings J_{FM} and J_{AFM} between the Gd moment and the substrate magnetization, since dipolar coupling between Ni and Gd spins plays only a minor role for the system under study [27]. Such a scenario implies different molecular species on the surface, which may be attributed to varying orientations of the C_{80} cage or distinct cage isomers [28]. If the larger number of Gd moments exhibit a weak antiferromagnetic coupling to the Ni film, whereas the remaining smaller number is ferromagnetically coupled, a behavior such as observed in Fig. 3(c) results. At low temperatures, where also a weak coupling leads to a high alignment of the moments, the coupling strength is less relevant, and the antiparallel alignment of the majority species dominates the net magnetization. At increasing temperature the difference in coupling strength between the two species becomes more and more important, such that the net magnetization is dominated by the species with the higher coupling energy.

The dashed lines in Fig. 3 result from a simultaneous fit of all data to a model with effective Hamiltonian

$$\mathcal{H} = -J_{\mathrm{Gd}} \sum_{i<j} \mathbf{J}_i \cdot \mathbf{J}_j + D \sum_{i=1}^{3} (\mathbf{e}_z \cdot \mathbf{J}_i)^2 - \mu_{\mathrm{B}} g \sum_{i=1}^{3} \mathbf{B} \cdot \mathbf{J}_i - J_{\mathrm{FM/AFM}} \sum_{i=1}^{3} \mathbf{m}_{\mathrm{Ni}} \cdot \mathbf{J}_i \quad (1)$$

for three magnetic moments of magnitude $J = 7/2$. The first, second, and third terms are the intramolecular exchange, anisotropy, and Zeeman terms discussed previously. The fourth term describes the exchange between the magnetization of the Ni substrate and the Gd atoms.

We take the FM exchange constant $J_{FM} > 0$ for a fraction f of the clusters, and the antiferromagnetic exchange constant $J_{AFM} < 0$ for the remaining fraction $1 - f$, so that the net magnetization $M = fM_{J_{FM}} + (1-f)M_{J_{AFM}}$. The substrate magnetization is assumed to be always saturated in the range of measurements, which is a simplification at grazing incidence and low magnetic fields [25,29]. In the fits J_{Gd} was taken to be independent of the choice of the substrate. We set the anisotropy $D_{Ni} = 0$ for $Gd_3N@C_{80}$ on Ni, and used $D = D_{Cu}$ as a free fit parameter for the Cu substrate. The parameters J_{FM} and J_{AFM} apply to the Ni substrate only. A simultaneous fit to the data then yields $J_{Gd} = 50\ \mu$eV, $f = 43\%$, $J_{FM} = 6.1$ meV, $J_{AFM} = -2.2$ meV, and $D_{Cu} = 25\ \mu$eV (dashed curves in Fig. 3).

As an alternative model, we consider the scenario that different Gd ions inside the same molecule couple differently to the substrate. Taking one out of the three Gd ions in a cluster to couple ferromagnetically, we replace the fourth term in Eq. (1) by $-J_{FM}\mathbf{m}_{Ni} \cdot \mathbf{J}_1 - J_{AFM}\mathbf{m}_{Ni} \cdot (\mathbf{J}_2 + \mathbf{J}_3)$. Fitting to this model gives $J_{Gd} = 137\ \mu$eV, $J_{FM} = 5.1$ meV, and $J_{AFM} = -2.0$ meV (Fig. 3). Note that any more complicated distribution of different coupling energies can of course also fit the data due to the larger number of parameters.

The presence of at least two different species of Gd atoms is corroborated by XMCD measurements. Figure 4 shows Gd M_5 XMCD signals measured in external magnetic fields of $B = 0.1$ and 5.9 T, reversed in sign and scaled to the same size. A distinct shift in energy and a concomitant increase in linewidth of the Gd M_5 XMCD peak is observed when increasing the magnetic field from 0.1 to 5.9 T. The XMCD signal results from a superposition of the contributions from both Gd species. At $B = 5.9$ T the moments of all species are aligned with the field and contribute to the spectrum, whereas at the small field of 0.1 T the XMCD peak is dominated by the contribution of the more strongly coupled species. The shift of the XMCD peak thus reflects different electronic ground states of the two species, despite their equivalent $4f^7$ configuration [30]. This is in line with $Gd_3N@C_{80}$ bulk measurements, which revealed the presence of two different Gd atoms with a different oxidation state at temperatures above 1.2 K [23].

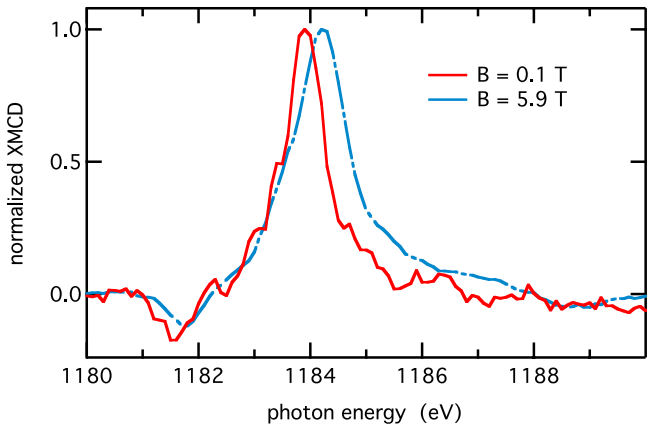

FIG. 4 (color online). Gd M_5 XMCD curves, scaled to +1 at the maximum, of $Gd_3N@C_{80}$ on Ni/Cu(001), recorded at normal incidence and $T = 4.5$ K in an external magnetic field of 0.1 T (red continuous line) and 5.9 T (blue broken line) applied along the incidence direction.

The magnetic coupling to the substrate, considering the encapsulated nature of the Gd atoms, must be based on an indirect carbon-cage-mediated exchange mechanism. Because of orbital hybridization between the guest lanthanide atoms and the carbon cage, a magnetic coupling has been suggested [9,31]. The orbitals of the cage are then likely to mediate the coupling to the substrate, similar to coupling across graphene [24].

Our theoretical model complies with different physical interpretations of this coupling. In a first scenario two types of molecules, each containing Gd atoms of the same electronic configuration, but with different geometric orientation of their encapsulated Gd clusters with respect to the carbon cage and/or the surface, are present on the surface. The different orientation would then result in a different coupling to the substrate. Different orientations of the molecular cages are in fact resolved in the STM image of Fig. 1. Additionally, different deformations of the carbon cage could also lead to different coupling. In an alternative scenario, Gd atoms with a different electronic configuration inside the same fullerene exist. They could result from a different bonding to the fullerene cage. Whereas the molecular orbitals of the free molecule are highly symmetric, the adsorption on the surface induces a splitting of the degenerate LUMO and LUMO+1 orbitals depending on the molecular orientation on the substrate (Fig. 1). This may enhance different electronic properties of the Gd atoms and/or a different orientation with respect to the substrate. Regardless of the exact mechanism, our data clearly prove the existence of a substrate-induced spin polarization of the Gd atoms.

In conclusion, Gd spins of adsorbed $Gd_3N@C_{80}$ molecules couple ferromagnetically to each other. Deposition of these molecules on Ni films induces a spin polarization of the Gd $4f$ magnetic moments, which is based on an indirect carbon-cage-mediated exchange coupling. At least two Gd species, having a different electronic ground state but the same $4f^7$ configuration, are found for the fullerenes on the surface. The magnetic moments of one of them couple parallel, the other antiparallel, to the Ni spins. While the latter dominate in percentage, the former exhibit a stronger coupling, such that at sufficiently low temperatures the resulting net Gd magnetization is aligned antiparallel with respect to the Ni magnetization. Also noteworthy is the demonstrated possibility to control the Gd net magnetization in size, orientation, and sign with respect to the substrate magnetization by varying the

temperature or the Ni magnetization by means of an externally applied magnetic field. We believe that such a magnetic substrate coupling is not only specific to the case of $Gd_3N@C_{80}$ but more generally valid likewise also for other, similar endohedral fullerenes. Our results thus constitute a step forward towards a future molecular spin electronics, by combining the magnetism of thin films and endohedral fullerenes.

E. Schierle is acknowledged for technical support. Funding by the DFG [Sfb 658 and the priority programme 1459 (M. S.)], the Alexander von Humboldt Foundation (P. W. B.), as well as the DAAD (G. A.) is gratefully acknowledged.

*kuch@physik.fu-berlin.de

[1] H. W. Kroto, J. R. Heath, S. C. O'Brien, R. F. Curl, and R. E. Smalley, Nature (London) **318**, 162 (1985).
[2] J. R. Heath, S. C. O'Brien, Q. Zhang, Y. Liu, R. F. Curl, F. K. Tittel, and R. E. Smalley, J. Am. Chem. Soc. **107**, 7779 (1985).
[3] M. Saunders, H. A. Jiménez-Vázquez, R. J. Cross, and R. J. Poreda, Science **259**, 1428 (1993).
[4] T. Almeida Murphy, Th. Pawlik, A. Weidinger, M. Höhne, R. Alcala, and J.-M. Spaeth, Phys. Rev. Lett. **77**, 1075 (1996).
[5] D. S. Bethune, R. D. Johnson, J. R. Salem, M. S. de Vries, and C. S. Yannoni, Nature (London) **366**, 123 (1993).
[6] S. Stevenson, G. Rice, T. Glass, K. Harich, F. Cromer, M. R. Jordan, J. Craft, E. Hadju, R. Bible, M. M. Olmstead, K. Maitra, A. J. Fisher, A. L. Balch, and H. C. Dorn, Nature (London) **401**, 55 (1999).
[7] R. Westerström, J. Dreiser, C. Piamonteze, M. Muntwiler, S. Weyeneth, H. Brune, S. Rusponi, F. Nolting, A. Popov, S. Yang, L. Dunsch, and T. Greber, J. Am. Chem. Soc. **134**, 9840 (2012).
[8] J. E. Grose, E. S. Tam, C. Timm, M. Scheloske, B. Ulgut, J. J. Parks, H. D. Abruña, W. Harneit, and D. C. Ralph, Nat. Mater. **7**, 884 (2008).
[9] A. Sebetci and M. Richter, J. Phys. Chem. C **114**, 15 (2010).
[10] F. Hajjaj, K. Tashiro, H. Nikawa, N. Mizorogi, T. Akasaka, S. Nagase, K. Furukawa, T. Kato, and T. Aida, J. Am. Chem. Soc. **133**, 9290 (2011).
[11] B. Náfrádi, Á. Antal, Á. Pásztor, L. Forró, L. F. Kiss, T. Fehér, É. Kováts, S. Pekker, and A. Jánossy, J. Phys. Chem. Lett. **3**, 3291 (2012).
[12] A. Scheybal, T. Ramsvik, R. Bertschinger, M. Putero, F. Nolting, and T. A. Jung, Chem. Phys. Lett. **411**, 214 (2005).
[13] H. Wende, M. Bernien, J. Luo, C. Sorg, N. Ponpandian, J. Kurde, J. Miguel, M. Piantek, X. Xu, P. Eckhold, W. Kuch, K. Baberschke, P. M. Panchmatia, B. Sanyal, P. M. Oppeneer, and O. Eriksson, Nat. Mater. **6**, 516 (2007).
[14] M. Bernien, J. Miguel, C. Weis, M. E. Ali, J. Kurde, B. Krumme, P. M. Panchmatia, B. Sanyal, M. Piantek, P. Srivastava, K. Baberschke, P. M. Oppeneer, O. Eriksson, W. Kuch, and H. Wende, Phys. Rev. Lett. **102**, 047202 (2009).
[15] M. Treier, P. Ruffieux, R. Fasel, F. Nolting, S. Yang, L. Dunsch, and T. Greber, Phys. Rev. B **80**, 081403 (2009).
[16] T. Huang, J. Zhao, M. Feng, A. A. Popov, S. Yang, L. Dunsch, and H. Petek, Nano Lett. **11**, 5327 (2011).
[17] M. Grobis, K. H. Khoo, R. Yamachika, X. Lu, K. Nagaoka, S. G. Louie, M. F. Crommie, H. Kato, and H. Shinohara, Phys. Rev. Lett. **94**, 136802 (2005).
[18] K. Muthukumar, A. Strozecka, J. Myslivecek, A. Dybek, T. J. A. Dennis, B. Voigtländer, and J. A. Larsson, J. Phys. Chem. C **117**, 1656 (2013).
[19] J. B. Goedkoop, B. T. Thole, G. van der Laan, G. A. Sawatzky, F. M. F. de Groot, and J. C. Fuggle, Phys. Rev. B **37**, 2086 (1988).
[20] Y. Teramura, A. Tanaka, B. T. Thole, and T. Jo, J. Phys. Soc. Jpn. **65**, 3056 (1996).
[21] M. C. Qian and S. N. Khanna, J. Appl. Phys. **101**, 09E105 (2007).
[22] M. Qian, S. V. Ong, S. N. Khanna, and M. B. Knickelbein, Phys. Rev. B **75**, 104424 (2007).
[23] L. Chen, E. E. Carpenter, C. S. Hellberg, H. C. Dorn, M. Shultz, W. Wernsdorfer, and I. Chiorescu, J. Appl. Phys. **109**, 07B101 (2011).
[24] C. F. Hermanns, K. Tarafder, M. Bernien, A. Krüger, Y.-M. Chang, P. M. Oppeneer, and W. Kuch, Adv. Mater. **25**, 3473 (2013).
[25] See Supplemental Material at http://link.aps.org/supplemental/10.1103/PhysRevLett.111.167203 for further experimental details, field-dependent XMCD measurements of the Ni film, sum-rule analysis of Gd magnetic moments, and linear dichroism of the Gd $M_{4,5}$ XA spectra.
[26] The Brillouin function with $J = 7/2$ yields only a magnetization between 0.001 and 0.002 relative to saturation in the temperature interval from 10 to 20 K, more than 1 order of magnitude less than the experimental data.
[27] Supplemental Material of Ref. [29].
[28] M. Krause and L. Dunsch, Angew. Chem., Int. Ed. **44**, 1557 (2005).
[29] A. Lodi Rizzini, C. Krull, T. Balashov, J. J. Kavich, A. Mugarza, P. S. Miedema, P. K. Thakur, V. Sessi, S. Klyatskaya, M. Ruben, S. Stepanow, and P. Gambardella, Phys. Rev. Lett. **107**, 177205 (2011).
[30] The absence of an appreciable linear dichroism of the Gd x-ray absorption spectroscopy signal [25] reflects the spherical symmetry of the probed unoccupied density of states, as expected for a pure $4f^7$ system with an open valence shell having atomic character.
[31] J. Lu, R. F. Sabirianov, W. N. Mei, Y. Gao, C. Duan, and X. Zeng, J. Phys. Chem. B **110**, 23 637 (2006).